Veterinary Microbiology 235 (2019) 301–309

Contents lists available at ScienceDirect

Veterinary Microbiology

journal homepage: www.elsevier.com/locate/vetmic

orf20 in prophage phiv142-3 contributes to the adhesion and colonization ability of avian pathogenic *Escherichia coli* strain DE142 by affecting the formation of flagella and I fimbriae

Dezhi Li[a], Yan Chen[a], Xinjie Qian[a], Yun Liu[a], Jianluan Ren[a], Feng Xue[a], Jianhe Sun[b], Fang Tang[a,*], Jianjun Dai[a]

[a] MOE Joint International Research Laboratory of Animal Health and Food Safety, Key Laboratory of Animal Bacteriology, Ministry of Agriculture, College of Veterinary Medicine, Nanjing Agricultural University, 210095 PR China
[b] Shanghai Key Laboratory of Veterinary Biotechnology, Shanghai, 200240, PR China

ARTICLE INFO

Keywords:
Avian pathogenic
Escherichia coli
Prophage
Flagella
I fimbriae
Colonization

ABSTRACT

We have previously demonstrated that prophage phiv142-3 enhances the colonization ability of avian pathogenic *Escherichia coli* (APEC) strain DE142. However, the mechanism of this action remains unknown. In this study, we demonstrate that deletion of phiv142-3 *orf20* leads to a decrease in the survival ability in chicken serum, adhesion, and ability to invade DF-1 cells of mutant strain DE142Δ*orf20* compared with that of wild type (WT). Avian infection assays showed that bacterial loads in lungs and hearts of chickens challenged with the mutant are decreased to 7% and 8.3% compared with those challenged with the WT. The number of flagella and I fimbriae of the mutant are decreased and the mutant exhibits filamentation. However, protein ORF20 shows no adhesion ability to DF-1 cells in adherence inhibition experiments, indicating that it does not directly participate in adhesion. qRT-PCR revealed that the deletion of *orf20* leads to reduction in the expression of nine genes related to the exportation of flagellar protein and two I-fimbriae-related genes (*fimA* and *fimH*), but does not affect genes related to the synthesis of flagella and other adhesins. Compared with the WT, the transcription level of the cell-division-associated genes *minC* and *minD* was increased 1.4-fold and 2.5-fold in mutant DE142Δ*orf20*, respectively, indicating that *orf20* affects the morphology of DE142 by regulating expression of *minC* and *minD*. Thus, our study revealed that *orf20* in prophage phiv142-3 played a role in flagellar exportation, cell morphology, and I fimbriae synthesis.

1. Introduction

Bacteriophages (phages) are viruses that infect bacteria. They are the most abundant biological entity in the biosphere with an estimated global population of 10^{31} (Wommack and Colwell, 2000). Depending on their lifestyle, phages can be divided into two categories: lytic phages, which utilizes the host cell machinery to accomplish phage replication, assembly, and the release of new generations after infecting bacteria; and temperate phages (prophages), whose DNA integrates into the bacterial genome or is maintained as an episome after infecting bacteria (Brussow et al., 2004). Most bacterial genomes contain up to 20% of the prophage sequence (Casjens, 2003).

To some extent, the survival of prophages relies on that of the host bacteria. In the form of bacterial lysogens, prophages are replicated together with the bacterial host chromosome. Thus, it is evolutionarily advantageous for prophages to encode genes that contribute to bacterial host cell fitness. The most well characterized advantage associated with prophages is the prevention of subsequent phage infection (Casjens, 2003). However, this is only one the most immediate effects. Prophages can also alter many of the traits of its host bacteria to enhance its survival or infection ability (Taylor et al., 2019). For example, prophages have been shown to increase bacterial swimming motility. It has been demonstrated that, after having obtained phage ϕMin27, bacterial flagellar biosynthesis genes are up-regulated, leading to improved swimming motility on semisolid agar, while non-flagellate mutants exhibit attenuated infection (Su et al., 2010). Furthermore, a number of studies on bacteria including *Pseudomonas aeruginosa* (Yu et al., 2015), *Ralstonia solanacearum* (Ahmad et al., 2017), and *Bacillus thuringiensis* (Gillis and Mahillon, 2014) confirm that prophages regulate bacterial motility.

* Corresponding author at: College of Veterinary Medicine, Nanjing Agricultural University, No.1 Weigang, Nanjing, 210095, Jiangsu province, PR China.
E-mail address: tfalice@126.com (F. Tang).

https://doi.org/10.1016/j.vetmic.2019.07.020
Received 21 May 2019; Received in revised form 17 July 2019; Accepted 20 July 2019

Being equipped with flagella allows the mother and daughter cells move efficiently after cell division and separation (Mears et al., 2014). In *E. coli*, the Min system plays a vital role in cell division and maintaining normal cell morphology (Taviti and Beuria, 2018). In addition, *dicB* of prophage Qin acts as an inhibitor of cell division in *E.coli* (Bejar et al., 1988). Furthermore, prophages can also participate directly in bacterial adhesion processes by encoding adhesins, such as B-cell-stimulating protein B (TspB) (Muller et al., 2013), which facilitates *Neisseria meningitidis* adhesion to tissue surfaces, and *E. coli* immunoglobulin binding protein (EibG) (Lu et al., 2006), which is found in a prophage of Shiga-toxin-producing *E. coli* and facilitates its adhesion to epithelial cells.

Avian pathogenic *E.coli* (APEC) strains cause avian colibacillosis, leading to significant economic loss in the poultry industry. APEC strain DE142, which belongs to serotype O2 and phylogenetic ECOR group B2, was first isolated from the brain of a duck exhibiting neurological symptoms. We have previously reported that the prophage phiv142-3 contributes to bacterial adhesion and colonization in DE142 (Li et al., 2018). However, the mechanism of this effect remains unknown. Accordingly, in the present study, the 54 genes in phiv142-3 are named after *orf1-orf54* according to the order from attL to attR and explored, and *orf20* was found to play an crucial role in pathogenicity using multiple approaches.

2. Materials and methods

2.1. Bacterial strains and culture

The bacterial strains and plasmids used in this study are listed in Table 1. All *E. coli* strains were grown in Luria-Bertani (LB) medium at 37 °C with aeration. Appropriate antibiotics [ampicillin (Amp, 100 μg mL^{-1}), kanamycin (Kan, 50 μg mL^{-1}), and chloramphenicol (Cm, 30 μg mL^{-1})] were added to the LB medium when necessary.

2.2. Construction of the knockout mutant and complement strains

The knockout mutant was constructed using the lambda red recombinase system described previously (Datsenko and Wanner, 2000). The *orf20* gene was replaced with a Kan resistance cassette, which contained upstream and downstream sequences of *orf20* and was amplified using plasmid pKD4 as a template. The mutants were verified by PCR and sequencing. PCR was performed using primers K1 and K2 combined with primers T-*orf20*-1 and T-*orf20*-2, and the PCR products were sequenced. In order to remove the Kan resistance gene, plasmid pCP20 was transferred into the mutant. Finally, the strain was subcultured serially in LB at 42 °C to remove pCP20, which was confirmed by PCR using primers pCP20-F and pCP20-R. Thus we got DE142Δ*orf20* and the other deletion mutant. The primers used are listed in Table 2 and Table S1.

To construct the complementation strain, the *orf20* sequence and its putative promoters were amplified. The product was sub-cloned into the pSTV-28 vector and the resulting plasmid was transferred into the mutant strain to generate the complementation strain DE142Δ*orf20/orf20**. The other complementation strain (DE142Δphiv142-3/*orf1-orf6**, DE142Δphiv142-3/*orf7-orf11**, DE142Δphiv142-3/*orf12-orf15**, DE142Δphiv142-3/*orf16-orf19**, DE142Δphiv142-3/*orf20-orf24**, DE142Δphiv142-3/*orf25-orf27**, DE142Δphiv142-3/*orf28-orf32**, DE142Δphiv142-3/*orf33-36**, DE142Δphiv142-3/*orf43-orf46**, DE142Δphiv142-3/*orf47-orf52**) were generated in similar fashion.

Table 1
Bacterial strains and plasmids used in this study.

Strains and plasmids	Description	Reference
DE142	APEC strain, O2 serotype	This study
DE142Δ*orf20*	orf20 deletion mutant	This study
DE142Δ*orf20/orf20**	Complementation strain	This study
pKD46	express λ red recombinase, Amp	(Datsenko and Wanner, 2000)
pKD4	template plasmid, Kan	(Datsenko and Wanner, 2000)
pCP20	yeast Flp recombinase gene, FLP, Cm, Amp	Takara
pSTV28	Expression using lac promotor, Cm	Takara

2.3. Bacterial growth curves

For the growth experiments, a single colony of each *E. coli* strain was selected and cultured overnight at 37 °C. The OD_{600} values were normalized to 1.0 with fresh LB, followed by sub-culturing in LB medium (1:100). The OD_{600} value of the bacterial culture was monitored with shaking (180 rpm) at 37 °C. The experiments were performed in triplicate.

2.4. Observation by electron microscopy

Bacterial culture lines were drawn on LB agar plates, which were then incubated at 37 °C for 12 h. Bacterial colonies were then suspended in doubly deionized H_2O, transferred onto a copper grid, and subjected to negative staining with phosphotungstic acid (PTA, 2%, *w/v*). Cell morphology was observed using an H 7650 transmission electron microscope (TEM; Hitachi, Japan)

2.5. Soft agar plate motility assay

Bacterial motility assays were performed using Petri dishes containing semisolid LB agar as previously reported (Wolfe and Berg, 1989). *E. coli* strains grown to the log phase were adjusted to an OD_{600} of 1.0 with fresh LB media. Then, a 10 μL aliquot of each suspension was injected into the center of an agar plate. After incubation at 37 °C for 12 h, the migration diameter of the bacterial cells was measured. Each strain was evaluated in three independent experiments.

2.6. Adhesion and invasion assays

Cell adhesion assays were performed as previously described (Wang et al., 2014). Chicken embryo fibroblast DF-1 cell monolayers were cultured in Dulbecco's modified Eagle's medium (DMEM) with 10% fetal bovine serum (without antibiotics) at 37 °C with a 5% CO_2 humidified atmosphere. Before each experiment, cells were sub-seeded in sterile 24-well-plates with 1×10^5 cells per well. Cultures of APEC strains DE142 and derivative strains were cultured overnight in 5 mL LB medium at 37 °C with shaking at 180 rpm. Cultures were then diluted 1:100 with fresh LB and grown at 37 °C with shaking at 180 rpm until the OD_{600} reached 0.6. Bacteria were then centrifuged at 5000 × g for 10 min and washed with DMEM. Then, bacteria were added to the wells with a multiplicity of infection (MOI) of 100. After centrifuging at 800 × g for 10 min, the plate was incubated at 37 °C with 5% CO_2 for 2 h to allow for cell adhesion. Then, the nonadherent (planktonic) bacteria were discarded. Ice-cold PBS was used to wash the adherent bacteria. For adhesion assays, cells were lysed with 0.5% Triton X-100. The number of adherent bacteria was quantified by the plate counting method. The experiments were performed in triplicate.

For invasion assays, after washing with PBS twice, the extracellular bacteria on the surface of the DF-1 cells were eliminated by adding gentamicin (50 μg mL^{-1}). After washing twice with ice-cold PBS, the cells were lysed with 0.5% Triton X-100 and the bacteria that had invaded them was counted by plating on LB plates. The experiments were performed in triplicate.

Table 2
Primers used in this study.

Primer	Sequence (5' to 3')	Target gene
K1	CAGTCATAGCCGAATAGCCT	pKD4
K2	CGGTGCCCTGAATGAACTGC	pKD4
Kt	CGGCCACAGTCGATGAATCC	pKD4
pKD46-F	GATACCGTCCGTTCTTTCCTT	pKD46
pKD46-R	TGATGATACCGCCTGCCTTACT	
pCP20-F	ATTGGGTACTGTGGGTTTAGTGGTT	pCP20
pCP20-R	TTGGCTTATCCCAGGAATCTGTC	
*orf20*Mu-F	TGCTGCGGCTGTTGCCAATATTGGACAGCGCACGATTGCAGATCTCTACTACAGAGGCCAGTGTAGGCTGGAGCTGCTTC	pKD4
*orf20*Mu-R	GGGCGTGTAAGCCTCGCGGATCAGACAAGGGGCTTCGGCCCCTTTATTGCAGGAGTGTATCATATGAATATCCTCCTTAG	
T-*orf20*-1	GGCGGTGGATTGCTCGTA	*orf20*
T-*orf20*-2	AAAATCATCAACGATGTG	
RT-*fimA*-F	GTTGTTCTGTCGGCTCTGTC	*fimA*
RT-*fimA*-R	TAAAGTGAACGGTCCCACCA	
RT-*fimH*-F	CTTATGGCGGCGTGTTATCT	*fimH*
RT-*fimH*-R	CGGCTTATCCGTTCTCGAATTA	
RT-*aufG*-F	CTGGATCAGCAACCTGGATATT	*aufG*
RT-*aufG*-R	CCCACACATCCGGCATATTA	
RT-*csgC*-F	TTCCAGTCAGATAACCTT	*csgC*
RT-*csgC*-R	ACAGACAAGATTGAGTAAG	
RT-*yqiL*-F	AGATCAGACGGTGAACTTTGG	*yqiL*
RT-*yqiL*-R	TCCCGTAATCACATAGCGTAAAT	
RT-*flhA*-F	GTCGCCCAGGAGATGCCAAA	*flhA*
RT-*flhA*-R	CATGTTCCGCCAGCGTTTCG	
RT-*flhB*-F	CGCGTTCCCGTGAACTGACT	*flhB*
RT-*flhB*-R	CGGAGAGCATGCCCGACAAT	
RT-*fliH*-F	TGATAATCTGCCGTGGAA	*fliH*
RT-*fliH*-R	GCCTCTTCAATAATGGTTTCT	
RT-*fliI*-F	GTGTTGCTGATTATGGACTC	*fliI*
RT-*fliI*-R	CGACGGTGGATAACCTTTA	
RT-*fliJ*-F	GCAATAACCTCAATAGCGATA	*fliJ*
RT-*fliJ*-R	TTCTGCGTCCACTGATTA	
RT-*fliO*-F	TGGAAGATGCACGGCTGGTG	*fliO*
RT-*fliO*-R	TCCCGCCACGCTTAAGCAAA	
RT-*fliP*-F	CTGTCGCACCGGTCCTTCTC	*fliP*
RT-*fliP*-R	GGAGCGACCAGCTTTGTCCA	
RT-*fliQ*-F	CGCTGGTCACGGGCCTTATC	*fliQ*
RT-*fliQ*-R	GCATCCACGGTCCGGCAATA	
RT-*fliR*-F	CGCGCCAATTCTGAGCGAAC	*fliR*
RT-*fliR*-R	GGCCAGCCACAGAGCAAAGA	
RT-*minD*-F	CAGTATTGCGCGCCTCTAA	*minD*
RT-*minD*-R	CTTCTCCCAACAGACGTTCTAC	
RT-*minC*-F	CGTTCCGGTCAGCGTATTTA	*minC*
RT-*minC*-R	CATGAATGTTACCATCGGCAATC	

2.7. Adherence inhibition experiments

The adherence inhibition assays were performed as previously described (Dai et al., 2010). Approximately 50 μg of purified protein ORF20 was added to DF-1 monolayer dishes and incubated for 1 h. DF-1 cells incubated with 50 μg bovine serum albumin (BSA) were used as a control. After 1 h incubation at 37 ℃, PBS was used to wash out the protein form the DF-1 monolayer dishes, and the bacteria were added to the dishes according to adherence assay procedures.

2.8. Bacterial colonization during systemic infection

Forty chickens (seven days old) obtained from a poultry farm in Jiangsu province and that tested negative for antibodies to APEC DE142 were used in this study. The *orf20* mutant strain, complemented strain, and wild type (WT) DE142 strain were cultured overnight (16–18 h) followed by sub-culturing (1:100) into LB medium until the OD_{600} reached 0.6. The bacteria were then washed twice with ice-cold PBS. The chickens were divided into four groups. Three groups of 10 chickens each were challenged intratracheally with the WT, mutant, or complement strains (2×10^7 CFU for each strain). The remaining 10 chickens were intratracheally injected with the same volume of PBS as a control group. At 24 h post-infection, chickens were euthanized and dissected. The organs were harvested and homogenized, and the bacterial loads in the heart, lung and liver tissues were calculated using LB agar plates. The assay was performed in triplicate with three independent experiments.

2.9. RNA isolation and qRT-PCR

The DE142 and DE142Δ*orf20* strains were grown to an OD_{600} of 0.6 in LB broth at 37 °C. Then, RNA was extracted from the bacteria using a Bacterial RNA Kit (OMEGA, Beijing, China). HiScript II Q RT SuperMix for qPCR + gDNA wiper (Vazyme Biotech) were used for reverse transcription. The mRNA transcription levels were determined using a One Step qRT-PCR SYBR Green Kit (Vazyme Biotech). The relative expression level of the genes were calculated by the $2^{-\Delta\Delta Ct}$ method. All date were normalized to the endogenous reference gene *DnaE*. Assays were performed three times. The primers used are listed in Table 2 and Table S1.

2.10. Survival in chicken serum

Chicken serum was obtained from specific-pathogen-free (SPF) chickens. A bactericidal assay was performed in 1.5 mL tubes as described previously (Wang et al., 2014) with some modifications. Briefly, SPF chicken serum was diluted to 50% in PBS. Approximately 100 μL of 5×10^7 CFU bacteria were added to 900 μL of the 50% serum. After

incubation at 37 °C for 30 min, bacterial numbers were evaluated using LB plates. The assay was performed in triplicate with three independent experiments.

2.11. Ethics statement

Animal experiments were performed in accordance with the guidelines of the Association for Assessment and Accreditation of Laboratory Animal Care International. The animal study protocol was approved by the Ethical Committee for Animal Experiments of Nanjing Agricultural University (SYXK(SU)2011-0036), Nanjing, China.

2.12. Statistical analyses

Statistical analyses were performed using the GraphPad Prism Software package (GraphPad Software, La Jolla, CA, USA). The Mann-Whitney *U* test was used for analysis of the data from *in vivo* colonization, and two-way ANOVA was used to assess the qRT-PCR results. Student's *t*-test was used for analysis of the rest of the data. Figures show mean values. Statistical significances were established at $P < 0.05$ and indicated by an asterisk (*).

2.13. Accession number

The sequence of *orf20* was deposited in the GenBank database (accession number MK940831).

3. Results

3.1. orf20–orf24 contributes to bacterial adherence in DE142

In this study, the phiv142-3 sequence was divided into 13 sections, including *orf1-orf6*, *orf7-orf11*, *orf12-orf15*, *orf16-orf19*, *orf20-orf24*, *orf25-orf27*, *orf28-orf32*, *orf33-orf36*, *orf37-orf39*, *orf40-orf42*, *orf43-orf46*, *orf47-orf52* and *orf53-orf54*. To identify which section plays an important role in adhesion *in vitro*, we attempted to transfer each of the 13 sections into DE142Δphiv142-3, obtaining 10 complementation strains (failed to obtain *orf37-orf39*, *orf40-orf42* and *orf53-orf54*). The adhesion ability of DE142Δphiv142-3 was increased by the plasmid carrying *orf20–orf24* (Fig. S1a). Therefore, we surmised that the *orf20–orf24* region contributed to bacterial adherence in DE142.

3.2. orf20 enhances the adhesion and invasion capacities of DE142

In order to identify which *orf* plays the key role in the fragment *orf20–orf24*, we knocked out each *orf* in the fragment and assessed the adhesion ability of each mutant (Fig. S1b). The adhesion ability of the *orf20* KO decreased most (85.2% reduction) among 5 *orf* KO (*orf20*, *orf21*, *orf22*, *orf23*, *orf24*). The adhesion and invasion ability of this mutant was decreased to 14.8% (Fig. 1a, $P < 0.001$) and 23.8% (Fig. 1b, $P < 0.001$) compared with that of the WT, respectively. Furthermore, the adhesion and invasion abilities were restored in the corresponding complementation strain.

3.3. The survival ability of the orf20 KO mutant in chicken serum is decreased

Through respiratory tract is the most common route for APEC infecting and invading the host and resultant septicemia. Thus, the ability to survive in chicken serum is important for APEC. Bactericidal assays performed with normal chicken serum revealed that the number of mutant cells decreased to 50.6% (Fig. 2a, $P < 0.05$) compared with WT. Furthermore, the resistance of the complementation strain to the serum was restored.

To investigated if *orf20* influence the expression level of the well-known genes related to serum resistance in *E.coli* (Mellata et al., 2003), qRT-PCR was used to determinate the transcription level of *ompA*, *bor* and K1 capsule related genes (*kpsF*, *kpsE*, *kpsC* and *kpsM*). The result showed that these genes (except *bor gene*) were down-regulated 2–4 fold in DE142Δ*orf20* (Fig. 2b). It suggested that the *orf20* gene in prophage phiv142-3 enhanced the bacterial survival ability in serum by up-regulating the expression of several serum resistance genes.

3.4. The colonization ability of the orf20 KO mutant in vivo is significantly decreased

The colonization ability of mutant DE142Δ*orf20* was assessed *in vivo*. Three groups of chickens were intratracheally injected with WT DE142, DE142Δ*orf20*, or complementation strains. The bacterial loads in the lung and heart tissues of the chickens challenged with the KO mutant decreased to 7% and 8.3% compared with those of the WT (Figs. 3a and 3b, $P < 0.05$). There was no significant difference in the liver tissue. The bacterial loads of the complementation strain were restored to those of the WT. Hence, *orf20* facilitated bacterial colonization and proliferation *in vivo*.

3.5. Protein ORF20 exhibits no adhesion ability to DF-1 cells

Adherence inhibition experiments were performed to investigate whether protein ORF20 directly participates the adhesion process. First, protein ORF20 can be detected by Western blot when DE142 was grown in LB (data not shown), suggesting that protein ORF20 was expressed in the WT. The DF-1 cells were pre-incubated with protein ORF20 and BSA. After washing out the nonadherent protein, the adherence ability of the WT to DF-1 cells was tested. The result showed that the number of DE142 cells adhered to DF-1 cells pre-incubated with protein ORF20

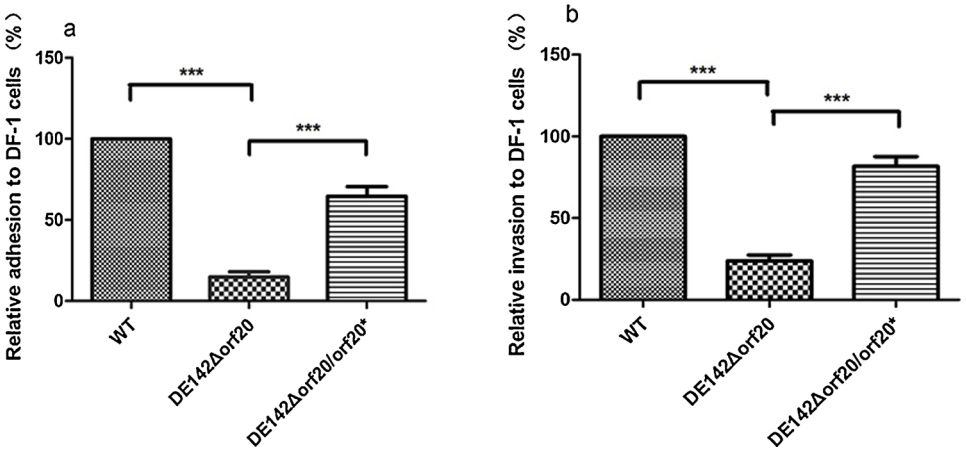

Fig. 1. Adhesion and invasion assay results. (**a**) Relative percentage of the strain that adhered to DF-1 cells. In adhesion assays, the 100% represents a 15% of inoculum of the WT. Values are the average of three independent experiments. Error bars indicate standard deviations. ***P < 0.001 (**b**) Relative percentage of the strain that invaded DF-1 cells. In invasion assays, the 100% represents a 0.1% of inoculum of the WT. Values are the average of three independent experiments. Error bars indicate standard deviations. ***$P < 0.001$.

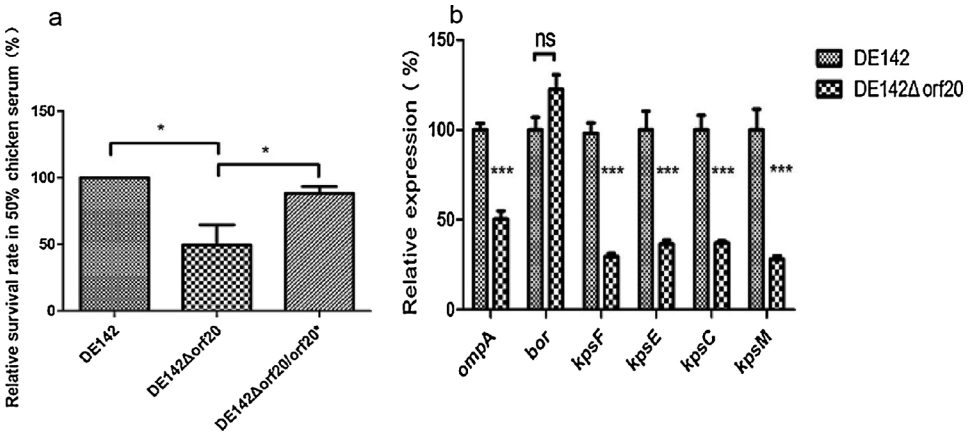

Fig. 2. Bacterial resistance to normal chicken serum. (**a**) The survial rate of the srains in 50% chicken serum. DE142Δ*orf20* shows significantly reduced resistance. One-way analysis was performed for significance. $^{*}P < 0.05$. (**b**) Quantification of genes related to serum resistance. Expression levels of *ompA*, *bor* and K1 capsule related genes (*kpsF*, *kpsE*, *kpsC* and *kpsM*) in strains DE142 (WT) and DE142Δ*orf20* were measured by qRT-PCR. The acquired cycle threshold (CT) was normalized to the CT of the housekeeping gene *dnaE*. Data are presented as the mean ± SD of three independent experiments, with each experiment being comprised of four individual measurements. Unpaired T-tests were performed for significance. $^{***}P < 0.001$.

was not significantly different to that of the negative control (DF-1 cells incubated with BSA) (Fig. S2), revealing that protein ORF20 had no adhesion ability to DF-1 cells.

3.6. orf 20 deletion leads to filamentation and decreases the number of flagella and fimbriae of the mutant

To investigate whether the decrease in the adhesion and colonization abilities of the mutant were attributed to changes in the flagella or fimbriae, the cell morphologies were observed using TEM (Fig. 4). A striking observation was that the mutant DE142Δ*orf20* was elongated (Fig. 4b), which appeared to be due to cell division inhibition. Furthermore, the number of flagella of the mutant was decreased compared with that of the WT (Figs. 4a and 4b). As flagella can easily detach off from the bacteria, we examined the deciduous flagella in the visual field. Far fewer deciduous flagella were observed for DE142Δ*orf20* (Fig. 4e) than for the WT (Fig. 4d). Flagella have a profound effect on the swimming motilities of bacteria, so the swimming motilities of different strains were measured by assessing the distance migrated from inoculation centers on semisolid LB agar plates. The results revealed that the diameter of the halo of the WT (1.12 cm) was larger than that of the mutant (1.03 cm) ($P < 0.05$), confirming that the decreased in flagella influences the swimming motility of the mutant. We also observed that the number of fimbriae decrease in the mutant (Fig. 4c).

The growths of different strains were also assessed. The results showed no significant differences (date not shown). These observations indicated that the decrease in the adhesion and colonization abilities of the mutants were due to the decrease in flagella or fimbriae.

3.7. orf20 contributes to the exportation of flagellar protein

To further figure out how *orf20* affects the number of flagella, the transcription levels of genes relative to flagella formation were screened by qRT-PCR. Flagella synthesis is regulated by a series of genes: Firstly, *flhDC* is a class I operon required for the expression of all other flagellar genes; secondly, class II operons consisting of flagellar hook-basal body components and the transcriptional regulator *fliA*; and thirdly, class III genes that encode flagellin, hook-associated proteins, and various chemotaxis proteins. The transcription levels of class I operon (*flhD* and *flhC*), class II operon (*fliA*, *fliS*, *flgM* and *fliD*) and class III operon (*fliC* and *flgE*) are slightly increased or decreased but not signifcantly (data not shown) in DE142Δ*orf20* compared to those in WT. The FliC protein is a flagellar filament structural protein. Thus, the expression levels of FliC in mutant and WT cells were assessed by Western blot, and the results indicate that there was no obvious difference in expression levels of FliC between the two strain (Fig. S3). Therefore, these results showed that *orf20* had no effect on the regulation and expression of genes related to synthesis of flagella, but the number of flagella decrease without *orf20*, suggesting that *orf20* might contribute to the exportation of flagella. To verify this, nine proteins (FliH, FliI, FliJ, FlhA, FlhB, FliO, FliP, FliQ and FliR) reported to be responsible for the exportation of flagellar protein were investigated by qRT-PCR. The results showed that these genes were down-regulated 2–4 fold in DE142Δ*orf20* (Fig. 5), confirming our assumption.

3.8. orf20 increases expression levels of fimA and fimH

To elucidate the mechanism by which *orf20* affected the number of fimbriae, the expression levels of I-fimbriae-related genes *fimA* and *fimH* were determined by qRT-PCR. As shown in Fig. 6, the expression

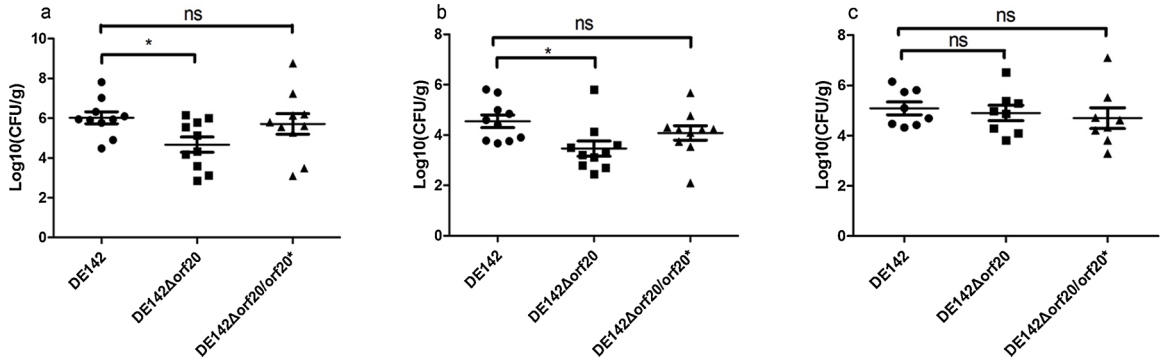

Fig. 3. Bacterial colonization during infection *in vivo*. Chickens were intratracheally infected with 2×10^7 CFU of WT DE142, DE142Δ*orf20*, or DE142Δ*orf20/orf20**. Bacterial re-isolation from the (**a**) lung, (**b**) heart, and (c) liver 24 h post-infection were quantified by the plate counting method. Each data point represents a sample from an individual chicken. Mann-Whitney *U* test was performed for significance. $^{*}P < 0.05$.

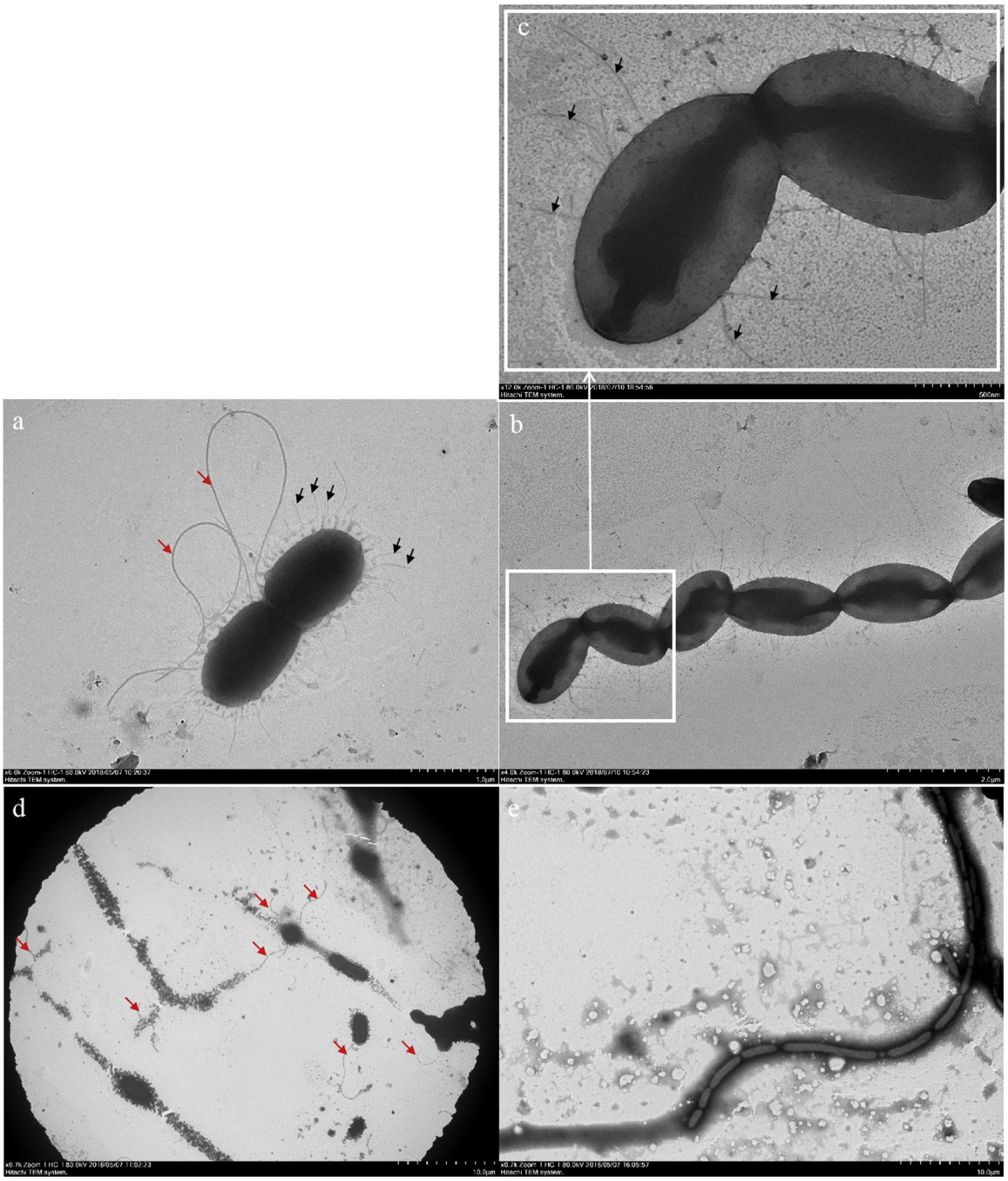

Fig. 4. Observation of bacterial morphology by TEM. DE142 produces flagella (red arrow) and I fimbria (black arrow) appendages on the outer membrane when cultured in LB static broth at 37 °C for 12 h. DE142Δ*orf20* does not produce flagella and produces less I fimbria on the outer membrane. Bacteria were negatively stained with 2% of phosphotungstic acid. (**a**) Morphology of the WT at cell division (×6000). (**b**) Morphology of DE142Δ*orf20* at cell division (×4000). (**c**) Morphology of DE142Δ*orf20* at cell division (×12,000). (**d**) WT flagella at low magnification (×700). (**e**) DE142Δ*orf20* at low magnification (×700) (For interpretation of the references to colour in this figure legend, the reader is referred to the web version of this article).

levels of *fimA* and *fimH* were decreased 66% and 53% in DE142Δ*orf20*, respectively.

To investigate whether the decrease in adhesion and colonization abilities of the KO mutant was caused by other adhesins, the adhesins *yqiL*, *csgC*, and *aufG* were also investigated by qRT-PCR (Fig. 6). The results showed no significant changes in the expression of these adhesins. Thus, *orf20* contributed to the adhesion and colonization of DE142 by increasing the expression levels of *fimA* and *fimH*.

3.9. The elongated morphology of DE142Δorf20 is due to up-regulation of minC and minD

DE142Δ*orf20* exhibits an elongated morphology, which we speculated might be related to cell division. The Min system, including *minC* and *minD*, is mainly responsible for cell division. Thus, the transcription levels of *minC* and *minD* were investigated by qRT-PCR (Fig. 7). Compared with those of WT, the transcription levels of *minC* and *minD* in mutant DE142Δ*orf20* were increased 1.4-fold and 2.5-fold, respectively, indicating that *orf20* affected the morphology of DE142 by regulating expression of *minC* and *minD*.

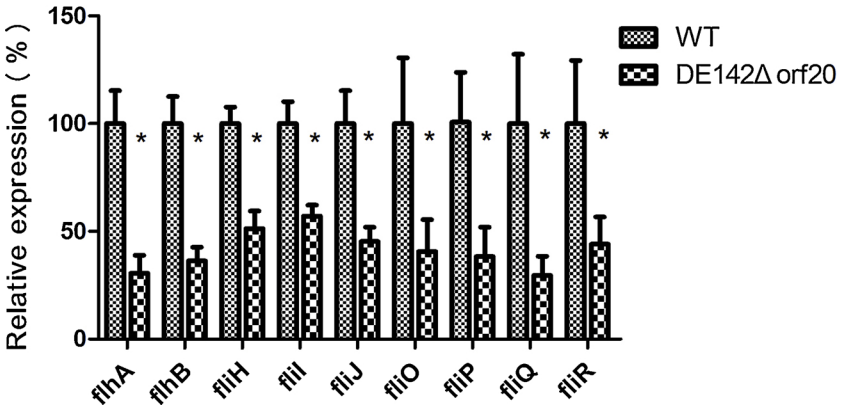

Fig. 5. Quantification of nine genes that code proteins related to the transportation of flagella. Expression levels of *flhA*, *flhB*, *fliH*, *fliI*, *fliJ*,*fliO*, *fliP*, *fliQ*, and *fliR* in strains DE142 (WT) and DE142Δ*orf20* were measured by qRT-PCR. The acquired cycle threshold (CT) was normalized to the CT of the housekeeping gene *dnaE*. Data are presented as the mean ± SD of three independent experiments, with each experiment being comprised of four individual measurements. Unpaired T-tests were performed for significance. $^{*}P < 0.05$.

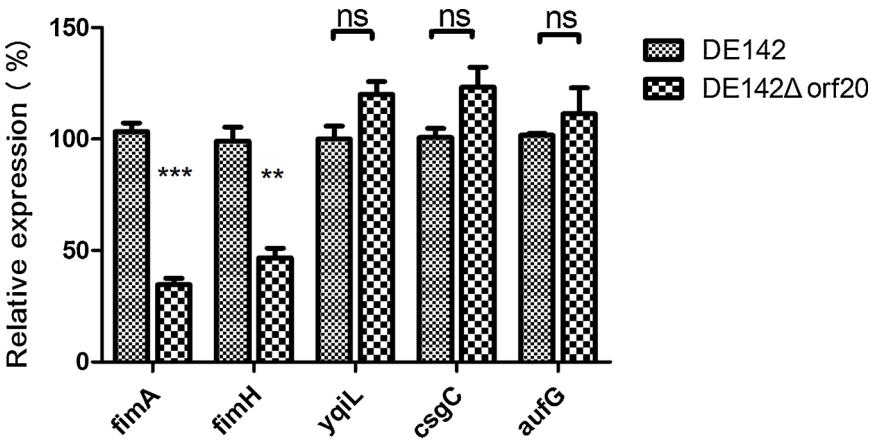

Fig. 6. Quantification of adhesins. Expression levels of *fimA*, *fimH*, *yqiL*, *csgC*, and *aufG* in WT DE142 and DE142 as measured by qRT-PCR. The acquired cycle threshold (CT) was normalized to the CT of the housekeeping gene *dnaE*. Data are presented as the mean ± SD of three independent experiments, with each experiment being comprised of four individual measurements. Unpaired T-tests were performed for significance. $^{***}P < 0.001$, $^{**}P < 0.01$.

4. Discussion

APEC infection is a common problem in the poultry industry worldwide, causing huge economic losses (Dho-Moulin and Fairbrother, 1999). Thus, improving our understanding of the pathogenic mechanism of APEC would be of enormous benefit to the poultry industry, aiding the control of APEC-related diseases. Previous study in our lab has revealed that prophage phiv142-3 aids bacterial colonization (Li et al., 2018). Our results in this study indicated that the ability of mutant strain DE142Δ*orf20* to colonize chicken lung and heart tissues is decreased compared with that of the WT.

APEC infects poultry by initial respratory tract colonization followed by bacteremia (Wang et al., 2014). The survival ability in the host serum is an improtant factors for APEC infection. The result showed that *ompA* and K1 capsule related genes were down-regulated 2–4 fold in DE142Δ*orf20* (Fig. 2b). This may be the reason that DE142Δ*orf20* showed a significantly reduced survival rate in SPF chicken serum and might subsequently lead to the decreased colonization *in vivo*.

Flagella have been demonstrated to mediate adhesion and invasion, and are also implicated in the virulence of pathogenic bacteria (Moens and Vanderleyden, 1996). As the number of flagella of the mutant are decreased compared with that of the WT, we investigated the transcription level of genes related to flagella synthesis. The mRNA levels of *flhD*, *flhC*, *fliA*, *flgM*, *fliT*, *flgE*, *fliC* and *fliS* in DE142Δ*orf20* showed no significant differences to those in WT. While flagellar exportation associated genes were significantly down-regulated in DE142Δ*orf20* (Fig. 5). Thus, *orf20* is thought to participate in flagellar exportation,

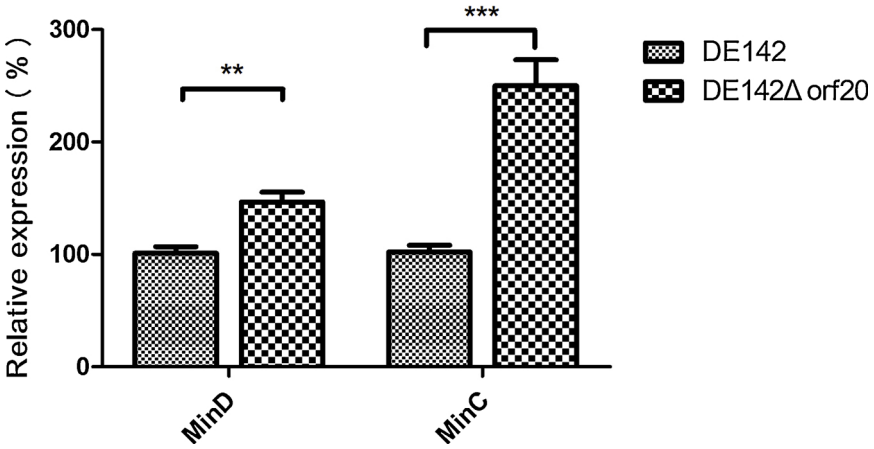

Fig. 7. Expression levels of *minD* and *minC* in WT DE142 and DE142Δ*orf20*. The mRNA levels were measured using qRT-PCR. The acquired cycle threshold (CT) was normalized to the CT of the housekeeping gene *dnaE*. Data are presented as the mean ± SD of three independent experiments, with each experiment being comprised of four individual measurements. Unpaired T-tests were performed for significance. $^{***}P < 0.001$, $^{**}P < 0.01$.

leading to regulation of the number of flagella, further contributing to adhesion and colonization of the strain. This finding corresponds with Luneberg's reports (Luneberg et al., 2001) concerning human pathogen *Legionella pneumophila*, in which the flagellum and lipopolysaccharides synthesis are regulated by the excision and reintegration of a prophage region.

An indispensable step in APEC infection is adhesion (Antao et al., 2009). The results revealed that the expression levels of *fimH* and *fimA* are significantly decreased in DE142Δ*orf20* compared with those in WT (Fig. 6). FimH and FimA are involved in the synthesis of I fimbriae. FimH is a receptor-specific adhesin of the type I fimbriae, and FimA is a subunit of type I fimbriae (Antao et al., 2009). These results correspond with the TEM observations that DE142Δ*orf20* forms fewer I fimbriae. Numerous studies have reported that prophages are associated with IV pilus biosynthesis (Chiang et al., 2008; Chung et al., 2014), while few studies have reported the relationship between prophages and I fimbriae. Chuang et al. (Chuang et al., 2008) constructed a transposon library by transposon mutagenesis technology, and then found that prophage Gifsy-2 minor tail protein mutant causes a decreased of I fimbriae in *Salmonella typhimurium*. We reasoned that *orf20* might play a similar role in I fimbriae biosynthesis.

A striking observation is that the mutant strain DE142Δ*orf20* cells are elongated and exhibit inhibited cell division. The Min system regulates cell division. It contains three gene products MinC, MinD, and MinE. MinC directly interacts with FtsZ, preventing Z-ring formation (Lutkenhaus, 2007). Thus, it is believed to inhibit division. Overexpression of MinC alone can cause filamentation (de Boer et al., 1990). MinD is an activator of MinC that greatly increases the division-inhibitory activity of MinC (Romberg and Levin, 2003). Cell division blocking caused by prophages has been reported previously. For example, in *Vibrio Cholerae* O1 strains (Hassan et al., 2010) (including strains AO12682, AO7543, and AV2684248), a deficiency of prophage CTX leads to filamentation. From a prophage on the *E. coli* chromosome (Qin), DicB can interact with MinC and inhibited division (Mulder et al., 1992). Here, the deletion of the *orf20* gene leads to the transcription levels of minD and minC increasing 1.4-fold and 2.5-fold compared to those in the WT (Fig. 7), resulting in the filamentation observed for DE142Δ*orf20*.

Furthermore, minD has been reported to maintain proper cell division, and that its deletion mutant form minicells and filaments, leading to a decreased adhesion ability in enterohemorrhagic *E.coli* (EHEC) (Parti et al., 2011). In the present study, the gene *minD* is upregulated and results in filamentation of DE142Δ*orf20*, which may also be a factor for the decreased adhesion ability. FlhG is responsible for regulating the number of flagella in *Clostridium jejuni*, *Bacillus subtilis*, and *Shewanella putrefaciens* (Schuhmacher et al., 2015). However, FlhG is absent in *E. coli*, but it is structurally similar to MinD (Taviti and Beuria, 2018), so we hypothesise that MinD might have a similar function in flagella synthesis.

In summary, the present study has revealed that the deletion of the prophage gene *orf20* leads to a decrease in the number of flagella and fimbriae *in vitro*, and colonization ability in chicken lung and heart tissue *in vivo*. Adhesion, usually mediated by fimbriae, allows bacteria to attach to host cells and infect them, while flagella-driven movement allows bacteria to spread to more favorable locations for colonization. Thus, our study revealed that *orf20* in prophage phiv142-3 may play a role in flagella exporting, maintenance of normal cell morphology, and influence I fimbriae synthesis.

Author contributions

Fang Tang conceived and designed the experiment. Dezhi Li, Yan Chen, Yun Liu and Xinjie Qian performed most of the experiments described in the manuscript. Feng Xue analyzed the experimental data. Jianluan Ren and Jianhe Sun helped with the experiments. Dezhi Li drafted the paper. Jianjun Dai provided valuable suggestions of the manuscript. All authors approved the final version of the manuscript.

Declaration of Competing Interest

No conflict. All authors have submitted the ICMJE Form for Disclosure of Potential Conflicts of Interest.

Acknowledgments

This study was supported by the Natural Science Foundation of Jiangsu Province (BK20180075), and the Foundation of Key Laboratory of Veterinary Biotechnology (No. klab201709), Shanghai, P.R. China, Youth Foundation of the National Natural Science Foundation of China (grant 31402213), and the Fund of Priority Academic Program Development of Jiangsu Higher Education Institutions (PAPD).

Appendix A. Supplementary data

Supplementary material related to this article can be found, in the online version, at doi:https://doi.org/10.1016/j.vetmic.2019.07.020.

References

Ahmad, A.A., Stulberg, M.J., Huang, Q., 2017. Prophage Rs551 and its repressor gene *orf14* reduce virulence and increase competitive fitness of its *Ralstonia solanacearum* carrier strain UW551. Front. Microbiol. 8, 2480.
Antao, E.M., Wieler, L.H., Ewers, C., 2009. Adhesive threads of extraintestinal pathogenic *Escherichia coli*. Gut Pathog. 1, 22.
Bejar, S., Bouche, F., Bouche, J.P., 1988. Cell division inhibition gene *dicB* is regulated by a locus similar to lambdoid bacteriophage immunity loci. Mol. Gen. Genet. 212, 11–19.
Brussow, H., Canchaya, C., Hardt, W.D., 2004. Phages and the evolution of bacterial pathogens: from genomic rearrangements to lysogenic conversion. Microbiol. Mol. Biol. Rev. 68, 560–602.
Casjens, S., 2003. Prophages and bacterial genomics: what have we learned so far? Mol. Microbiol. 49, 277–300.
Chiang, P., Sampaleanu, L.M., Ayers, M., Pahuta, M., Howell, P.L., Burrows, L.L., 2008. Functional role of conserved residues in the characteristic secretion NTPase motifs of the *Pseudomonas aeruginosa* type IV pilus motor proteins PilB, PilT and PilU. Microbiology 154, 114–126.
Chuang, Y.C., Wang, K.C., Chen, Y.T., Yang, C.H., Men, S.C., Fan, C.C., Chang, L.H., Yeh, K.S., 2008. Identification of the genetic determinants of *Salmonella enterica* serotype Typhimurium that may regulate the expression of the type 1 fimbriae in response to solid agar and static broth culture conditions. BMC Microbiol. 8, 126.
Chung, I.Y., Jang, H.J., Bae, H.W., Cho, Y.H., 2014. A phage protein that inhibits the bacterial ATPase required for type IV pilus assembly. Proc Natl Acad Sci U S A 111, 11503–11508.
Dai, J., Wang, S., Guerlebeck, D., Laturnus, C., Guenther, S., Shi, Z., Lu, C., Ewers, C., 2010. Suppression subtractive hybridization identifies an autotransporter adhesin gene of*E. coli* IMT5155 specifically associated with avian pathogenic *Escherichia coli* (APEC). BMC Microbiol. 10, 236.
Datsenko, K.A., Wanner, B.L., 2000. One-step inactivation of chromosomal genes in *Escherichia coli* K-12 using PCR products. Proc Natl Acad Sci U S A 97, 6640–6645.
de Boer, P.A., Crossley, R.E., Rothfield, L.I., 1990. Central role for the *Escherichia coli* minC gene product in two different cell division-inhibition systems. Proc Natl Acad Sci U S A 87, 1129–1133.
Dho-Moulin, M., Fairbrother, J.M., 1999. Avian pathogenic *Escherichia coli* (APEC). Vet. Res. 30, 299–316.
Gillis, A., Mahillon, J., 2014. Influence of lysogeny of Tectiviruses GIL01 and GIL16 on *Bacillus thuringiensis* growth, biofilm formation, and swarming motility. Appl. Environ. Microbiol. 80, 7620–7630.
Hassan, F., Kamruzzaman, M., Mekalanos, J.J., Faruque, S.M., 2010. Satellite phage TLCphi enables toxigenic conversion by CTX phage through dif site alteration. Nature 467, 982–985.
Li, D., Tang, F., Xue, F., Ren, J., Liu, Y., Yang, D., Dai, J., 2018. Prophage phiv142-3 enhances the colonization and resistance to environmental stresses of avian pathogenic *Escherichia coli*. Vet. Microbiol. 218, 70–77.
Lu, Y., Iyoda, S., Satou, H., Satou, H., Itoh, K., Saitoh, T., Watanabe, H., 2006. A new immunoglobulin-binding protein, EibG, is responsible for the chain-like adhesion phenotype of locus of enterocyte effacement-negative, shiga toxin-producing Escherichia coli. Infect. Immun. 74, 5747–5755.
Luneberg, E., Mayer, B., Daryab, N., Kooistra, O., Zahringer, U., Rohde, M., Swanson, J., Frosch, M., 2001. Chromosomal insertion and excision of a 30 kb unstable genetic element is responsible for phase variation of lipopolysaccharide and other virulence determinants in *Legionella pneumophila*. Mol. Microbiol. 39, 1259–1271.
Lutkenhaus, J., 2007. Assembly dynamics of the bacterial MinCDE system and spatial regulation of the Z ring. Annu. Rev. Biochem. 76, 539–562.
Mears, P.J., Koirala, S., Rao, C.V., Golding, I., Chemla, Y.R., 2014. *Escherichia coli* swimming is robust against variations in flagellar number. Elife 3, e01916.

Mellata, M., Dho-Moulin, M., Dozois, C.M., Curtiss 3rd, R., Brown, P.K., Arne, P., Bree, A., Desautels, C., Fairbrother, J.M., 2003. Role of virulence factors in resistance of avian pathogenic *Escherichia coli* to serum and in pathogenicity. Infect. Immun. 71, 536–540.

Moens, S., Vanderleyden, J., 1996. Functions of bacterial flagella. Crit. Rev. Microbiol. 22, 67–100.

Mulder, E., Woldringh, C.L., Tetart, F., Bouche, J.P., 1992. New minC mutations suggest different interactions of the same region of division inhibitor MinC with proteins specific for minD and dicB coinhibition pathways. J. Bacteriol. 174, 35–39.

Muller, M.G., Ing, J.Y., Cheng, M.K., Flitter, B.A., Moe, G.R., 2013. Identification of a phage-encoded Ig-binding protein from invasive *Neisseria meningitidis*. J. Immunol. 191, 3287–3296.

Parti, R.P., Biswas, D., Wang, M., Liao, M., Dillon, J.A., 2011. A *minD*mutant of enterohemorrhagic*E. coli* O157:H7 has reduced adherence to human epithelial cells. Microb. Pathog. 51, 378–383.

Romberg, L., Levin, P.A., 2003. Assembly dynamics of the bacterial cell division protein FTSZ: poised at the edge of stability. Annu. Rev. Microbiol. 57, 125–154.

Schuhmacher, J.S., Rossmann, F., Dempwolff, F., Knauer, C., Altegoer, F., Steinchen, W., Dorrich, A.K., Klingl, A., Stephan, M., Linne, U., Thormann, K.M., Bange, G., 2015. MinD-like ATPase FlhG effects location and number of bacterial flagella during C-ring assembly. Proc Natl Acad Sci U S A 112, 3092–3097.

Su, L.K., Lu, C.P., Wang, Y., Cao, D.M., Sun, J.H., Yan, Y.X., 2010. Lysogenic infection of a Shiga toxin 2-converting bacteriophage changes host gene expression, enhances host acid resistance and motility. Mol Biol (Mosk) 44, 60–73.

Taviti, A.C., Beuria, T.K., 2018. Bacterial Min proteins beyond the cell division. Crit. Rev. Microbiol. 1–11.

Taylor, V.L., Fitzpatrick, A.D., Islam, Z., Maxwell, K.L., 2019. The diverse impacts of phage morons on bacterial fitness and virulence. Adv. Virus Res. 103, 1–31.

Wang, S., Dai, J., Meng, Q., Han, X., Han, Y., Zhao, Y., Yang, D., Ding, C., Yu, S., 2014. DotU expression is highly induced during in vivo infection and responsible for virulence and Hcp1 secretion in avian pathogenic *Escherichia coli*. Front. Microbiol. 5, 588.

Wolfe, A.J., Berg, H.C., 1989. Migration of bacteria in semisolid agar. Proc Natl Acad Sci USA 86, 6973–6977.

Wommack, K.E., Colwell, R.R., 2000. Virioplankton: viruses in aquatic ecosystems. Microbiol. Mol. Biol. Rev. 64, 69–114.

Yu, Z.C., Chen, X.L., Shen, Q.T., Zhao, D.L., Tang, B.L., Su, H.N., Wu, Z.Y., Qin, Q.L., Xie, B.B., Zhang, X.Y., Yu, Y., Zhou, B.C., Chen, B., Zhang, Y.Z., 2015. Filamentous phages prevalent in *Pseudoalteromonas* spp. Confer properties advantageous to host survival in Arctic sea ice. ISME J. 9, 871–881.